The International Conference on Experimental Solid Mechanics and Dynamics
(*X-Mech-2012*)
March 6-7, 2012, Tehran, Iran
Center of Excellence in Experimental Solid Mechanics and Dynamics,
School of Mechanical Engineering, Iran University of Science and Technology

Analysis of some effective parameters on Stress Intensity factors in a Half-plane with vertical edge crack which is subjected to an Un-symmetrical tilted wedge by means of Digital Shearography

[1]D. Ghahremani-Moghadam*, [2]N. Soltani, [3]H. Sanati, [4]A. Mohammadpour, [5]Ali. Galehdari

[1]PhD Student, Mechanical Engineering Department, University of Ferdowsi of Mashhad, Azadi square, Mashhad, Iran,

[2]Professor, [3]M.Sc, Mechanical Engineering Department, University of Tehran, Amirabad, Tehran, Iran
[4]M.Sc, Metallurgy and Material Engineering Department, University of Tehran, Amirabad, Tehran, Iran
[5]PhD Student, Mechanical Engineering Department, University of Ferdowsi of Mashhad, Azadi square, Mashhad, Iran,
*(Tel: (98) 935 369 0689, e-mail: d.g.moghadam@gmail.com)

Abstract

Determination of Stress Intensity Factor is one of the important parameters in fracture mechanics. One of the common geometries in evaluating of fracture mechanics problems is contact of tilted wedge with half plane that in this article Unsymmetrical tilted wedge geometry has been studied and digital Shearography as a non-destructive technique is applied to determine mixed mode stress intensity factors in a half plane with vertical edge crack which is subjected to an unsymmetrical tilted wedge. Optical setup with two in-plane illumination source is used to determine purposed strain variable and consequently obtain the mixed mode stress intensity factors as a result of applying linear elastic fracture mechanics (LEFM). The results of Shearography technique contains some fringes which contain the information needed to obtain the strain variables. To utilize the advantage of whole field Shearography and to minimize random experimental errors, the least square method is used to obtain SIF. In order to verify the obtained results accuracy, the experimental results were compared with the results of finite element method. The difference between two results is nearly 19%. The comparison of the experimental results and the numerical results proves the credibility and potential of this non-destructive method in measurement applications. Then the effect of crack size and gap of tilted wedge from crack tip on Stress Intensity Factors have been investigated.
Finally it shown that in this problem Stress Intensity Factor in first mode of fracture is zero, so only second mode of fracture should be considered.

Keywords: Digital shearography; Tilted wedge; Half-plane; Stress Intensity Factor; Least Square Method

1. Introduction

Shearography is an interferometric technique for strain and deformation. It overmatches its predecessor holography in several aspects. Firstly, Shearography is a self-reference technique and requires no additional reference beam, which simplifies the optical setup. Greatly relaxes the vibration isolation requirement and make it suitable for applications in hostile environment. Secondly, Shearography enable direct measurement of strain, which makes it insensitive to the disturbance of rigid body movement and being appropriate for debonds and cracks detection since flows in material cause strain concentration. Thirdly, Shearography optical setup is simple and it is convenient to pack up a miniature instrument for handy in-situ application. Due to these distinct advantages Shearography is obtaining more and more acceptance in industry as well as in laboratory since its invention. During the last few decades, quit a large amount of research work regarding Shearography has been conducted. The invention of the first working laser by Theodore H.Maiman in 1960 opens a door to coherent optical metrology. Since then, a series of interferometric optical measuring techniques such as holographic interferometry [1], Shearography [2], moire' interferometry [3] and speckle metrology [4] bloomed to enrich the field of experimental mechanics greatly. Shearography, being one of the most widely applied experimental techniques today, was named in 1982. It grew from conventional Shearography using portrait camera as recording media to TV Shearography which directly displays the resultant fringes on a TV screen and finally to the current digital Shearography which involves automatic phase evaluation and enables quantitative analysis of speckle gram. In the present work Shearography was used for determination of mixed mode SIFs in Half-plane with vertical edge crack which is subjected to an Un-symmetrical tilted wedge Furthermore, FEM simulation of contact problem between a Half-plane with vertical edge crack and a tilted wedge is done and the experimental results compared with FEM results.

2. Basis of Digital Shearography Technique

Shearography technique is one of the optical interference techniques, except that in other techniques interference of waves is conducted through collision of a reference light mass with released waves from the body surface, but in this technique the conducted interference is due to shearing of images in a shearing device. Shearing device can be a glass wedge or a Michelson interferometer, “Figure 1”.

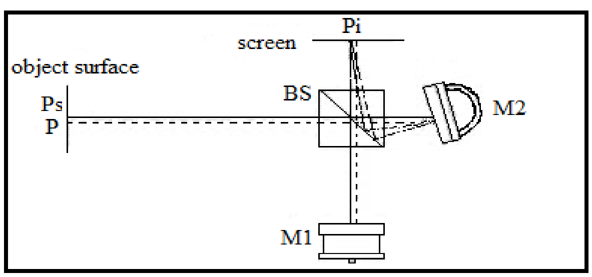

Figure1: Schematic of waves' interference in Michelson interferometer [3].

As it is obvious in “Figure 1”, Michelson interferometer consists of two mirrors M1 and M2 with vertical axes and a laser beam splitter. In this system the released beams from two points P and P_s of body surface interfere with each other in point P_i of screen. Also, with rotation of mirror 2 under a small angle a pair of sheared image from object surface is consisted in the camera. Due to interference of two sheared images a speckle pattern is obtained.

3. Phase Fringes Pattern Relations

It is clear that by applying a speckle pattern in shearography technique the desired solutions cannot be obtained, so in this technique after applying deformation in object surface, another speckle pattern is provided too and by exerting correlation of two patterns the desired mechanical relations are obtained.

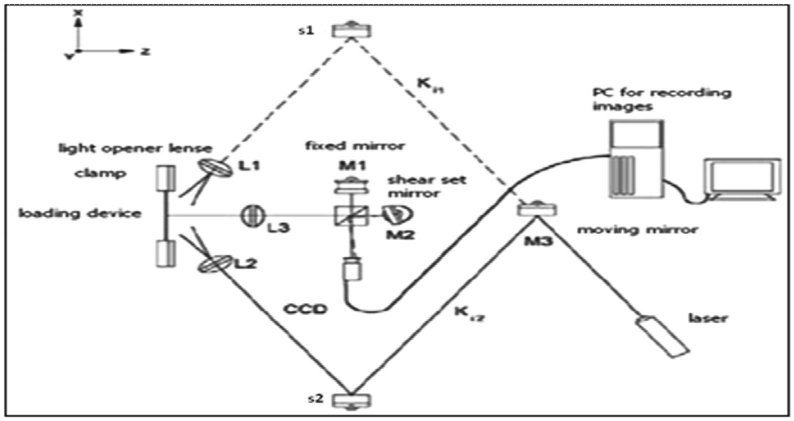

Figure2: Used digital shearography configuration in test.

To obtain stress intensity factors, two elements of in-plane strain $\frac{\partial u}{\partial x}$ and $\frac{\partial v}{\partial y}$ should be defined by test.To achieve this goal, in this study by using configuration with bi-directional radiation(figure3), at any stage of the body status, four images are taken as follows:

1. The first image by making a horizontal shear with size of Δx, source S1 (first light source), axis x as horizontal,
2. The second image by making a horizontal shear with size of Δx, source S2 (second light source), axis x as horizontal,
3. The third image by making a vertical shear with size of Δy, source S1, axis y as horizontal , and
4. The fourth image by making a vertical shear with size of Δy, source S2, axis y as horizontal.

It is worth mentioning that axis x is along with width of object and axis y is along with length of object. Now by applying mutual correlation of corresponding images, before and after loading, four phase fringe patterns are obtained.

With a simple subtraction of the phase patterns before and after loading, two desired elements can be obtained as follows:

$$B_1 - B_2 : \Delta j_x = \Delta j_1 - \Delta j_2 = 2K_x \frac{\partial u}{\partial x} \Delta x \quad (1)$$

$$B_3 - B_4 : \Delta j_y = \Delta j_3 - \Delta j_4 = 2K_x \frac{\partial v}{\partial y} \Delta y \quad (2)$$

In above relations, values B correspond with phase fringes pattern in each stage, K_x is radiation wave vector with size of $\frac{2p}{l}$ in which laser wavelength l has been applied. The object rotation has been $\frac{p}{2}$ around z axis.

As mentioned before, to obtain phase fringes pattern in each stage a computer program has been written, using MATLAB software environment.

4. Experimental procedure

The experiment includes nine test cases that were run by three specimens under different load (Table1).

Table1: Associated specimen and loading of the test cases

Case	Specimen No.	Loading(kgf)
1	1	3.75
2	1	10.1
3	1	18.8
4	2	3.75
5	2	10.1
6	2	18.8
7	3	3.75
8	3	10.1
9	3	18.8

The scheme and geometrical specifications of the specimens and un-symmetrical tilted wedge are detailed in fig.4. Young's modulus of elasticity and Poisson's ratio of plexiglas is 3.34 (Gpa) and 0.33, respectively. The wavelength of the employed He-Ne laser is 632.8(nm). In all test cases the amount of shear was 1mm (in this example $\Delta y = 1mm$). The speckle pattern images taken by the digital camera were recorded and saved on a computer that is shown in fig 4. For case 2 subtraction before and after loading images, the fringe demonstration $\frac{\partial u}{\partial x}$ appear. For typical case 2 experimental shearographic fringes is demonstrated in fig 5.

Table 2: Geometric specifications of specimens.

Specimen No.	Width, w(mm)	Crack length, a(mm)	Thickness, h(mm)	Length, L(mm)
1	60	4	5	240
2	60	5	5	240
3	60	6	5	240

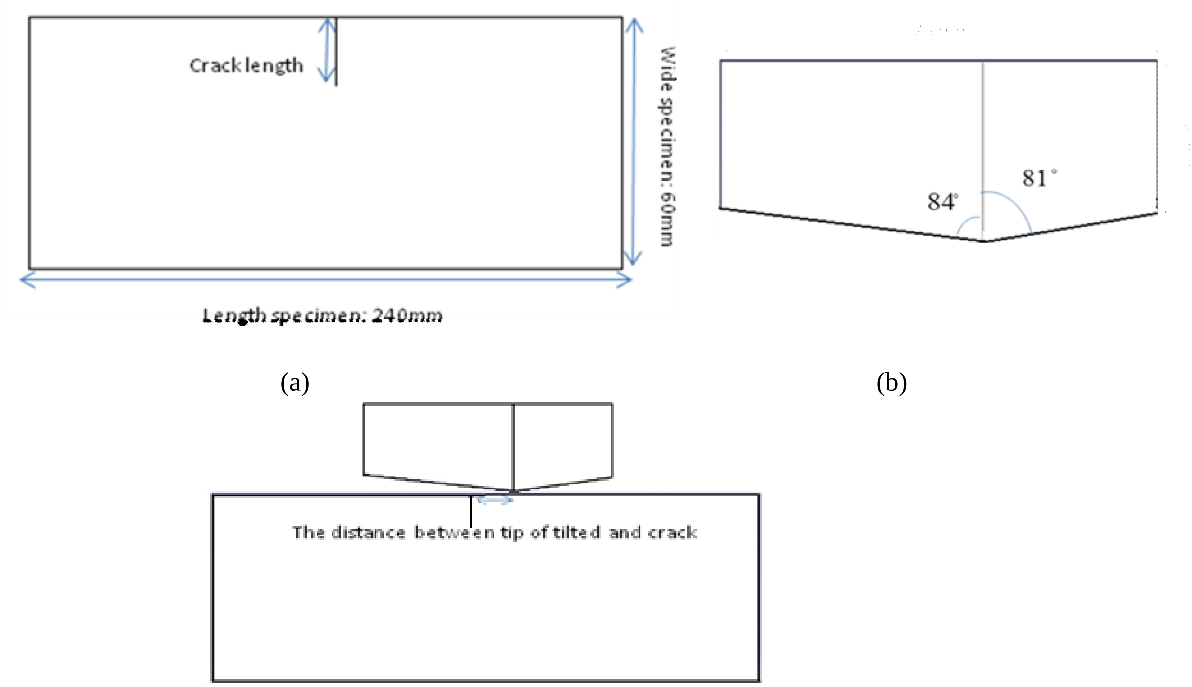

(a) (b)

(c)

Figure3: (a): Provided specimens for test, (b): Un-symmetry tilted and its geometric properties, (c): Type of tilted location on half-plane

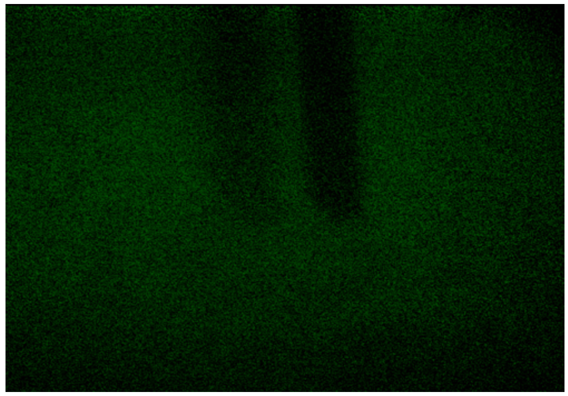

Figure4: the speckle pattern images taken by the digital camera

Figure5: experimental shearographic fringes for typical case 2

5. Numerical solution

A finite element model of the specific geometry is constructed, and then is analyzed with ABAQUS 6.7. Element CPE4R are used to represent the tilted wedge and half plane. The x-axis of the half-plane represents the contact surface. Finite Sliding Formulation is used for contact condition between tilted wedge and half plane. The half-plane and tilted wedge have a modulus of Elasticity of 3.34 (Gpa) and Poisson's ratio of 0.33. The normal and tangential forces are applied on the tilted wedge and the coefficient of the friction is non-zero. Strain derivative contours at the vicinity of the tip in X direction are displayed in “Figure 6”.

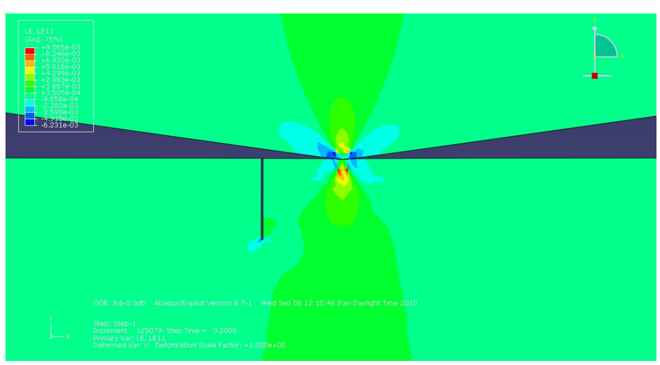

Figure 6: strain derivative contours at the vicinity of the tip in X direction

6. Determination of K_I and K_{II} values using Digital Shearography results

By means of mechanical relation at each point regarding "Figure 7":

$$s_X + s_Y = s_x + s_y \tag{3}$$

And also:

$$s_x + s_y = \frac{E}{1-n}(e_x + e_y) \tag{4}$$

So we have:

$$s_X + s_Y = \frac{E}{1-n}(e_x + e_y) = \frac{E}{1-n}\left(\frac{\partial u}{\partial x} + \frac{\partial v}{\partial y}\right) \tag{5}$$

According to relations governing fracture mechanic [6] in the vicinity the tip of crack, s_x, s_y for a specimen with a crack which undertakes would be:

$$(s_X)_{\mathrm{I}} = \frac{K_{\mathrm{I}}}{\sqrt{2pr}}\cos\left(\frac{q}{2}\right)\left(1 - \sin\frac{q}{2}\sin\frac{3q}{2}\right) \tag{6}$$

$$(s_X)_{\mathrm{II}} = -\frac{K_{\mathrm{II}}}{\sqrt{2pr}}\sin\left(\frac{q}{2}\right)\left(2 + \cos\frac{q}{2}\cos\frac{3q}{2}\right) \tag{7}$$

$$(s_Y)_{\mathrm{I}} = \frac{K_{\mathrm{I}}}{\sqrt{2pr}}\cos\left(\frac{q}{2}\right)\left(1 + \sin\frac{q}{2}\sin\frac{3q}{2}\right) \tag{8}$$

$$(s_Y)_{\mathrm{II}} = \frac{K_{\mathrm{II}}}{\sqrt{2pr}}\cos\left(\frac{q}{2}\right)\sin\left(\frac{q}{2}\right)\cos\left(\frac{3q}{2}\right) \tag{9}$$

Substituting Eqs (6-9) into Eq (5) in plane strains in the vicinity the tip of the crack would be:

$$\frac{2}{\sqrt{2pr}}\left[K_{\mathrm{I}}\left(\cos\left(\frac{q}{2}\right)\right) - K_{\mathrm{II}}\left(\sin\left(\frac{q}{2}\right)\right)\right] = \frac{E}{1-n}\left(\frac{\partial u}{\partial x} + \frac{\partial v}{\partial y}\right) \tag{10}$$

Since the illumination angle in -45° as a result we find:

s_0

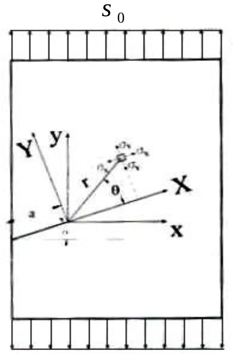

s_0

Figure 7: location of Cartesian coordinate systems x-y and X-Y with respect together on tip of a diagonally edge crack of specimen

$$\Delta j_x = -\frac{4p}{l} \times \frac{\sqrt{2}}{2} \times \frac{\partial u}{\partial x} \times \Delta x \tag{11}$$

And for shearing in y direction considering $a = 45^{\circ}$:

$$\Delta j_y = \frac{4p}{l} \times \frac{\sqrt{2}}{2} \times \frac{\partial v}{\partial y} \times \Delta y \tag{12}$$

In plane strains as a function of phase of selected points can be obtained from Eqs (11-12):

$$\frac{\partial u}{\partial x} = -\frac{\Delta j_x}{\frac{2p}{l} \cdot \sqrt{2} \cdot \Delta x} \tag{13}$$

$$\frac{\partial v}{\partial y} = \frac{\Delta j_y}{\frac{2p}{l} \cdot \sqrt{2} \cdot \Delta y} \tag{14}$$

Substituting Eqs(13-14) in Eq (10), the stress intensity factors dependency to phase of points takes the form:

$$\frac{2}{\sqrt{2pr}}\left[K_{\mathrm{I}}(\cos(\frac{q}{2})) - K_{\mathrm{II}}(\sin(\frac{q}{2}))\right] = \frac{E}{(1-n)\cdot\frac{2p}{l}\cdot\sqrt{2}}\left(-\frac{\Delta j_x}{\Delta x} + \frac{\Delta j_y}{\Delta y}\right) \tag{15}$$

Although two data points are sufficient to determine K_{I} and K_{II} but in order to take advantage of whole field shearography and increase the accuracy, the data for several points are registered and least square method is utilized [7]. Then K_{I} and K_{II} are obtained as:

$$\begin{Bmatrix} K_I \\ K_{II} \end{Bmatrix} = \frac{1}{\left(\frac{2}{p}\sum\frac{1}{r_i^2}\cos^2(\frac{q_i}{2})\right)\left(\frac{2}{p}\sum\frac{1}{r_i^2}\sin^2(\frac{q_i}{2})\right) - \left(\frac{1}{p}\sum\frac{1}{r_i^2}\sin(q_i)\right)^2} \begin{bmatrix} \frac{2}{p}\sum\frac{1}{r_i^2}\sin^2(\frac{q_i}{2})\cdot\frac{El}{(1-n)\cdot 2p\sqrt{p}}\sum\left(-\frac{(\Delta j)_{xi}}{\Delta x}+\frac{(\Delta j)_{yi}}{\Delta y}\right)\cdot\cos(\frac{q_i}{2}) - \frac{1}{p}\sum\frac{1}{r_i^2}\sin(q_i)\cdot\frac{El}{(1-n)\cdot 2p\sqrt{p}}\sum\left(-\frac{(\Delta j)_{xi}}{\Delta x}+\frac{(\Delta j)_{yi}}{\Delta y}\right)\cdot\sin(\frac{q_i}{2}) \\ -\frac{2}{p}\sum\frac{1}{r_i^2}\cos^2(\frac{q_i}{2})\cdot\frac{El}{(1-n)\cdot 2p\sqrt{p}}\sum\left(-\frac{(\Delta j)_{xi}}{\Delta x}+\frac{(\Delta j)_{yi}}{\Delta y}\right)\cdot\sin(\frac{q_i}{2}) + \frac{1}{p}\sum\frac{1}{r_i^2}\sin(q_i)\cdot\frac{El}{(1-n)\cdot 2p\sqrt{p}}\sum\left(-\frac{(\Delta j)_{xi}}{\Delta x}+\frac{(\Delta j)_{yi}}{\Delta y}\right)\cdot\cos(\frac{q_i}{2}) \end{bmatrix} \tag{16}$$

The SIF values are obtained for nine cases as given in "Table 3". These SIF values are compared against those obtained through numerical solution.

Table3: Comparison of numerical and digital Shearography SIFs.

Case	$K_{Shearography}(Mpa\sqrt{m})$	$K_{numerical}(Mpa\sqrt{m})$	difference (%)
1	8.23	6.81	16.4
2	34.42	28.12	18.2
3	43.52	35.33	18.7
4	19.82	16.01	19.2
5	45.38	35.48	21.8
6	64.93	50.3	22.5
7	27.1	21.9	19
8	51.04	40.55	20.5
9	76.1	58.61	23

Although as the Table 3 indicates the accuracy of the approach, there are some differences due to a few error sources which follows: The distance between crack tip and data points is too small to measure accurately, and locating exact position of the crack tip on images is to some extent troublesome. Furthermore the cracks were created by a 0.2 mm thick ring saw blade which created by tips instead of sharp. Also the laser beam may be not fully coherent.

7. Effect of crack size on the stress intensity factor

The effect of crack size in two states with different length of cracks according to specifications in Table 4 has been studied. In first state, crack length has changed between 0.2 to 1 mm and its related results are given in Figure 8. The investigated specifications in the second state are as Table 4 except the difference that crack size has changed between 3 to 6 mm and the distance of wedge tip to crack is 6 mm and the results of this study are shown in Figure 9.

It can be seen that in both states stress intensity factors in the second mode of failure increase with increase of crack length. Also in the second state that cracks length are larger, on contrary to the first state, by increase of crack length, tendency of crack edges increases to be closed and larger negative values for stress intensity coefficients in the first mode in this state are obtained.

Table 4: Problem Specifications.

Unit	Size	Parameter
degree	1.5	wedge bisector angle with vertical line
Degree	164	wedge total angle
-	0.1	friction factor
Kilonewton	37.5	Vertical force
Degree	90	crack angle with vertical line
millimeter	0.5	Crack size
Giga pascal	3.24	elasticity module
-	0.33	Poisson ratio
Millimeter	0.5	distance of crack to wedge tip

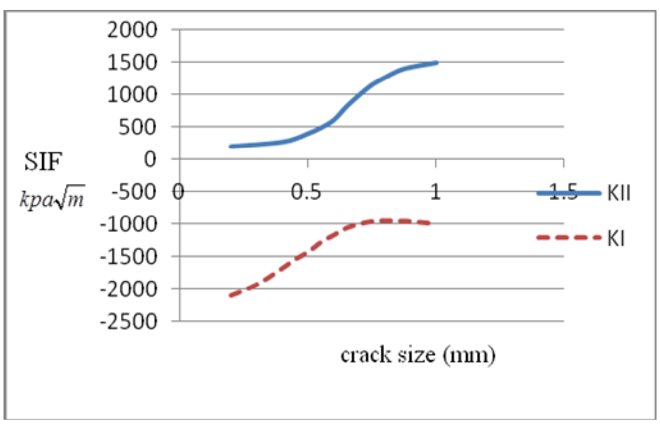

Figure**8:** Changes in stress intensity factor according to crack size in the first state.

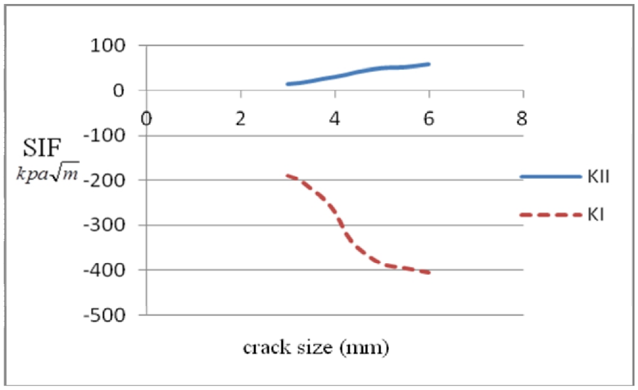

Figure**9:** Changes in stress intensity factor according to crack size in the second state.

8. Effect of crack location

To review the effect of crack location on stress intensity factors, the crack location has been displaced near the wedge tip to 1 mm beyond the contact area.
The problem specifications that are studied in this section are like Table 4 and distance of wedge tip from crack has changed from 0.25 to 2.75 mm and the results related to the effect of crack location are shown in Figure 10. It is seen that in this state by wedge move away from crack, stress intensity factor in the second mode and in other words the tendency of crack edges to slide on each other is reduced. Also the stress intensity factor in the first mode decreases in the negative state i.e. by increase wedge distance from the crack the tendency of crack edges to be closed decreases.

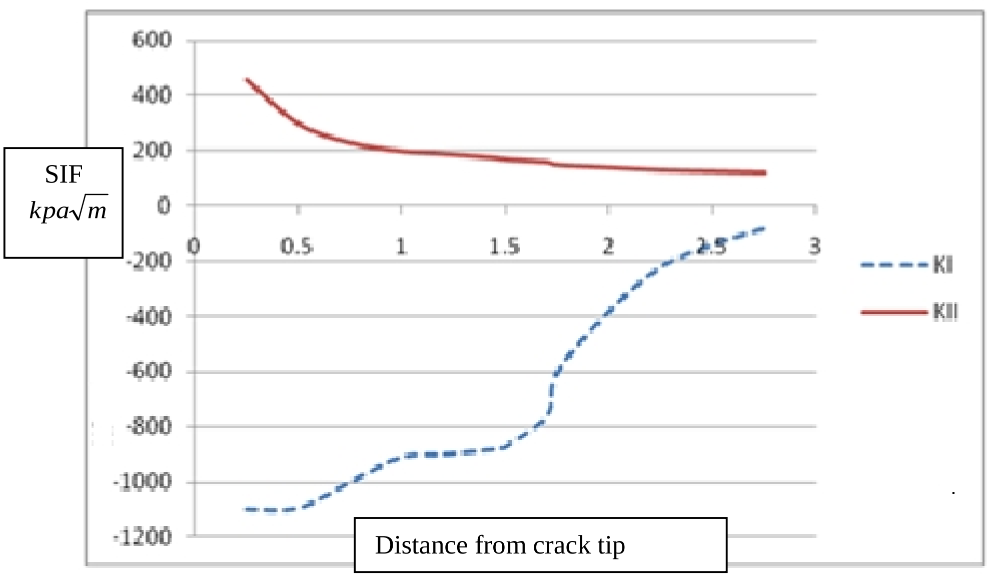

Figure10: Changes in stress intensity factors according to distance of wedge tip from crack

It is seen that in this state by wedge move away from crack, stress intensity factor in the second mode and in other words the tendency of crack edges to slide on each other is reduced. Also the stress intensity factor in the first mode decreases in the negative mode i.e. by increase wedge distance from the crack the tendency of crack edges to be closed decreases.

9. Conclusions

In this paper the contact problem between a tilted wedge and half-plane has been solved experimentally and numerically. Comparing the experimental and numerical values, the credibility and generality of SIF values are obtained for a cracked specimen by means of non-destructive technique of digital shearography. This comparing shows that the experimental results are reliable. Maximum percentage of the differences was 23%, Table 3 shows that for small loads the differences is lower.
Finally, by using the results obtained and due to assumptions used in problems solving mentioned, the following results are extractable:

- In all states the existing stress is compressive in the plane so the value of KI is zero.
- In this problem because the value of KI is zero, the life limiting factor is value of KII.
- In the second mode stress intensity factor increases by increase of crack length.
- By increase of wedge distance from crack, the value of stress intensity factors increases.

Acknowledgments

This research was supported by Research council of university of Tehran under grate no.8106027/1/02 which is gratefully acknowledgment.

References

[1] P.K.Rastogi (ed), 1994. Holographic interferometry : principles and methods. Berlin, Springer.
[2] W. Steinchen and L.X.Yang, 2003. Digital Shearography: theory and application of digital speckle pattern shearing interferometry. Bellingham, SPIE Optical Engineering press.
[3] D. Post, B. Han and P. Ifju, 1994 .High sensitivity moiré: experimental analysis for mechanics and materials. New York, Springer-Verlag.
[4] R.S. Sirohi(ed) , 1993 .Speckle metrology. New York, Marcel Dekker.
[5] M. Lehmann, 1998 . " Statistical theory of Two Wave Speckle Interferomatry and Its Application to the optimization Measurements ". M.Sc. Theses, Sciences Techniques, EPF Lausanne, No. 1797, Civil Eng. Dept., de-genie, Lausanne.
[6] D.Broek, 1991 .Elementary Eng. Fracture Mechanics. 4th Edition, Kluwer Academic Publisher, Dordrecht, Holland.
[7] A. Ghazavizadeh, N. Soltani, B.Hakimelahi, M.Ghasemieh, March. 2006. "Determination of Opening Mode Stress Intensity Factor for Edge Crack by Means of Digital Shearography Including Analytical and Numerical Simulations". Mech. & Aerospace Eng. J. Vol. 1 , No. 3